PROCEEDINGS OF SCIENCE

Searches for Supersymmetry with the ATLAS and CMS detectors

Vasiliki A. Mitsou[a,b,*] **on behalf of the ATLAS and CMS Collaborations**

[a] *Instituto de Física Corpuscular (IFIC), CSIC – Universitat de València, C/ Catedrático José Beltrán 2, E-46980 Paterna (Valencia), Spain*

[b] *Department of Physics, National and Kapodistrian University of Athens, University Campus, GR-15784 Zografou, Athens, Greece*

E-mail: vasiliki.mitsou@ific.uv.es

Supersymmetry (SUSY) provides elegant solutions to several problems in the Standard Model, and searches for SUSY particles are an important component of the LHC physics program. This paper presents the latest results from SUSY searches conducted by the ATLAS and CMS experiments with the Run 2 dataset. These searches target multiple final states and different assumptions about the decay mode of the produced SUSY particles, including searches for both R-parity conserving models and R-parity violating models and their possible connections with the recent observation of the flavour and muon $g-2$ anomalies. The paper also covers recent CMS and ATLAS SUSY searches for long-lived particles, targeting either the long-lived particle itself or its decay products at a significant distance from the collision point. These signatures provide interesting technical challenges due to their special reconstruction requirements as well as their unusual backgrounds.

*Corfu Summer Institute 2022 "School and Workshops on Elementary Particle Physics and Gravity", 28 August - 1 October, 2022
Corfu, Greece*

*Speaker

PoS(CORFU2022)074

1. Introduction

Supersymmetry (SUSY) [1–4] is an extension of the Standard Model (SM) which assigns to each SM field a superpartner field with a spin differing by a half unit. SUSY provides elegant solutions to several open issues in the SM, such as the hierarchy problem [5], the identity of dark matter [6], and the grand unification of fundamental interactions [7].

SUSY searches in collider experiments typically focus on events with high transverse missing momentum ($E_{\mathrm{T}}^{\mathrm{miss}}$) which can arise from the (weakly interacting) lightest supersymmetric particle (LSP), in the case of R-parity-conserving (RPC) SUSY, or from neutrinos produced in LSP decays, when R-parity is violated (RPV). Hence, the event selection criteria of inclusive channels are based on large $E_{\mathrm{T}}^{\mathrm{miss}}$, no or few light leptons (e, μ), many jets and/or b-jets, τ-leptons and photons. The exact sets of selection criteria (*signal regions*, SRs) are a compromise between the necessity to suppress events coming from known SM processes while maintaining a statistically sufficient number of surviving SUSY events. Typical SM backgrounds are top-quark production — including single-top —, W/Z in association with jets, dibosons and QCD multi-jet events. These are estimated using semi- or fully data-driven techniques in so-called *control regions* (CRs). Less dominant backgrounds are estimated by Monte Carlo (MC) simulation. Although the various analyses are motivated and optimised for a specific SUSY scenario or topology, the interpretation of the results may be extended to various SUSY or other beyond-SM (BSM) models, hence both collaborations are investing huge effort to facilitate the reinterpretation of their search results [8].

A summary of results from searches for SUSY with and without R-parity conservation is presented. The reported results are based on up to $\sim$ 140 fb^{-1} of data from proton–proton collisions at a centre-of-mass energy of $\sqrt{s}$ = 13 TeV recorded by ATLAS [9] and CMS [10] during Run 2 (2015–2018) at the Large Hadron Collider (LHC) [11]. Recent results from searches mainly targeting strongly produced sparticles, including third-generation squarks, are presented in Section 2, whilst electroweak (EW) production of EW gauginos and higgsinos ($\tilde{\chi}^0$, $\tilde{\chi}^\pm$) and sleptons ($\tilde{\ell}$) are discussed in Section 3. In Section 4, recent developments on the long-lived-sparticle front are highlighted. Lastly, Section 5 provides a summary of the results and an outlook.

2. Strong production including third-generation squarks

The production of the supersymmetric partners of quarks and gluons (squarks and gluinos) is characterised by large cross-sections at the LHC. Strong SUSY production is searched in events with large jet multiplicities and high missing transverse momentum, with and without leptons. Various channels fall into this class of searches; here several searches are showcased, some of which also target EW production of sparticles.

The mixing of left- and right-handed gauge states which provides the mass eigenstates of the scalar quarks and leptons can lead to relatively light 3$^{\mathrm{rd}}$ generation particles. Stop ($\tilde{t}_1$) and sbottom ($\tilde{b}_1$) with a sub-TeV mass are favoured by the naturalness argument [5, 12], while the stau ($\tilde{\tau}_1$) is the lightest $\tilde{\ell}$ in many models. Therefore, these sparticles could be abundantly produced either directly or through $\tilde{g}$ production and subsequent decay. Such events are characterised by several energetic jets (some of them b-jets), possibly accompanied by light leptons, as well as large $E_{\mathrm{T}}^{\mathrm{miss}}$.

2.1 One-lepton channel with W-boson and top-quark tagging

Events with a single electron or muon and multiple jets are selected in a CMS analysis with tagging of the W-boson and the top-quark [13]. Top-quark and W-boson identification algorithms based on machine-learning techniques are employed to suppress the main background contributions. Various exclusive search regions are defined that differ in the number of jets, the number of b-tagged jets, the number of hadronically decaying top quarks or W bosons, the scalar sum of all jet transverse momenta, H_{T}, and the scalar sum L_{T} of $E_{\mathrm{T}}^{\mathrm{miss}}$ and the lepton transverse momentum.

To reduce the main background processes from $t\bar{t}$ and W+jets production, the presence of a lepton produced in the leptonic decay of a W boson in the event is exploited. Under the hypothesis that all of the $E_{\mathrm{T}}^{\mathrm{miss}}$ originates from the neutrino produced in a leptonic W boson decay, the W boson momentum is calculated. The requirement of a large azimuthal angle, $\Delta\phi$, between the directions of the lepton and of the reconstructed W boson decaying leptonically, notably reduces the background contributions, as shown in Figure 1.

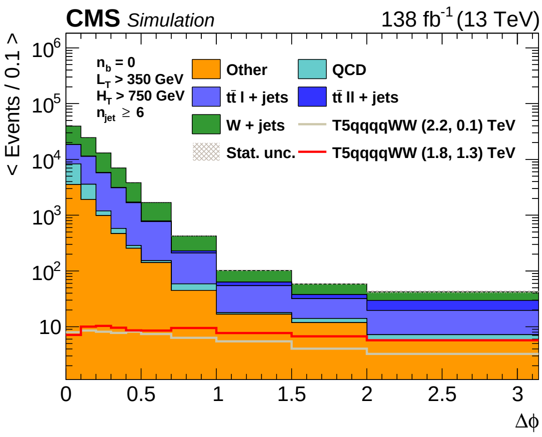

Figure 1: Signal and background distributions of the $\Delta\phi$ variable for the CMS one-lepton zero-b analysis, requiring at least six jets, $L_{\mathrm{T}} > 350$ GeV, $H_{\mathrm{T}} > 750$ GeV. The predicted signal distributions are also shown for two representative combinations of (gluino, neutralino) masses with large $(2.2, 0.1)$ TeV and small $(1.8, 1.3)$ TeV mass differences. From [13].

The event yields observed in data are consistent with the expectations from the SM processes, which are estimated with data in specific CRs. Exclusion limits on the sparticle masses in the context of two simplified models of gluino pair production are evaluated. Exclusions for gluino masses reach up to 2130 (2280) GeV at 95% confidence level (CL) for a model with gluino decaying to a $t\bar{t}$ pair (a $q\bar{q}$ pair and a W boson) and the LSP. For the same models, limits on the mass of the LSP reach up to 1270 (1220) GeV. This corresponds to an improvement on gluino (neutralino) masses by about 380 (270) GeV in comparison with the previous result [14], extending the existing limit from ATLAS [15] on the neutralino mass in the compressed region by about 150 GeV.

2.2 Two-leptons final state with edge in the $m_{\ell\ell}$ distribution

This ATLAS analysis presents searches for new phenomena in final states with exactly two oppositely charged same-flavour leptons, jets and $E_{\mathrm{T}}^{\mathrm{miss}}$ [16], which applies a shape fit [17] in the dilepton invariant mass, $m_{\ell\ell}$, distribution. The analysis is split into three searches probing both strong and EW sparticle production. Two searches target the pair production of charginos and neutralinos. One uses the recursive-jigsaw reconstruction (RJR) technique to follow up on excesses observed in 36.1 fb^{-1} of data [18] and the other uses conventional event variables. The third search targets pair production of coloured SUSY particles (squarks or gluinos) decaying through the next-to-lightest neutralino ($\tilde{\chi}_2^0$) via a slepton ($\tilde{\ell}$) or a Z-boson into $\ell^+\ell^-\tilde{\chi}_1^0$ resulting in a kinematic endpoint or peak in the $m_{\ell\ell}$ spectrum, depicted in Figure 2.

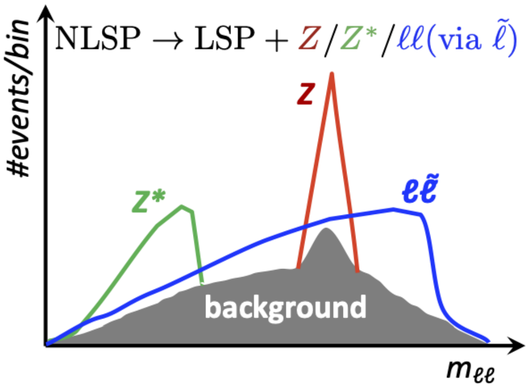

Figure 2: Schematic graph of the shape of the $m_{\ell\ell}$ distributions for leptonically decaying on-shell Z (red), off-shell Z^* (green) production and slepton-mediated NLSP decay (blue) to two leptons over the SM background (grey area).

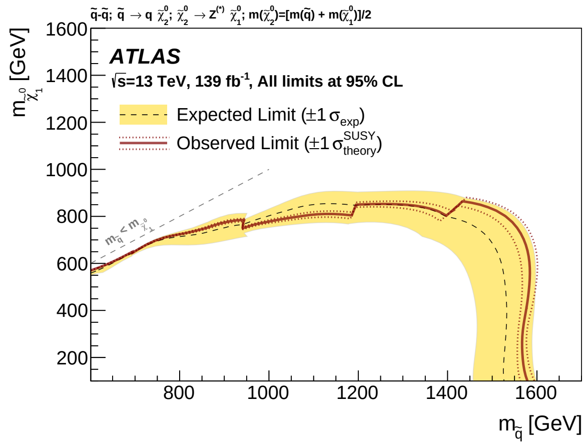

Figure 3: 95% CL expected and observed exclusion contours from the combination of all SRs for the $\tilde{q}$–Z model. The dashed line and yellow band indicate the expected limit and the 1σ experimental uncertainties. The red dotted lines around the observed limit indicate the signal cross-section uncertainty. From [16].

The data are found to be consistent with SM expectations and strong limits are set on possible BSM contributions to the SRs. The RJR search does not see significant excesses above the background expectation, thus the small excesses in the two-lepton channel of the 36 fb^{-1} dataset [18] did not persist with more data. The EW and strong searches results are interpreted with SUSY-inspired simplified models and set exclusion limits, expanding the sensitivity reach compared to previous ATLAS [19–21] and CMS [22] analyses. The EW search targets chargino-neutralino production and a gauge-mediated SUSY breaking (GMSB) model with higgsino next-to-the-lightest supersymmetric particles (NLSPs). Limits up to 820 GeV and 900 GeV are set on the masses of the mass-degenerate chargino-neutralino and higgsino NLSP, respectively. The strong search targets gluino or squark pair production, which decay via a Z boson or the NLSP, to lepton pairs and jets. Limits up to 2250 GeV and 1550 GeV are set on the masses of the gluino and squarks, respectively, as shown in Figure 3. Compared to the previous result [21], the limits of the gluino mass improved by 400 GeV and the limits of squark masses by 300 GeV. Improvements to both the strong and EW searches result from the increased size of the dataset and subsequent optimisations of analysis requirements.

2.3 Production of two top squarks with four-body decay

A search for the direct pair production of top squarks ($\tilde{t}_1$) in single-lepton final states has been carried out by CMS [23] within a compressed scenario where the mass difference $\Delta m = m(\tilde{t}_1) - m(\tilde{\chi}_1^0)$ between the lightest top squark and the neutralino LSP does not exceed the W boson mass. The considered decay mode of the top squark is the prompt four-body decay to $bf\bar{f}'\tilde{\chi}_1^0$, where the fermions in the final state f and f' represent a charged lepton and its neutrino for the decay products of one $\tilde{t}_1$, and two quarks for the other $\tilde{t}_1$. The search is based on data collected during 2017 and 2018, combined with the results from 2016 data [24]. Events are selected containing a single lepton (electron or muon), at least one high-$p_{\rm T}$ jet, and significant $E_{\rm T}^{\rm miss}$. The analysis is based on a multivariate boosted decision tree (BDT) specifically trained for different Δm regions, thus adapting the signal selection to the evolution of the kinematical variables as a function of $(m(\tilde{t}_1), m(\tilde{\chi}_1^0))$. An example of the BDT-output distributions for data, SM processes and a benchmark point are provided in Figure 4.

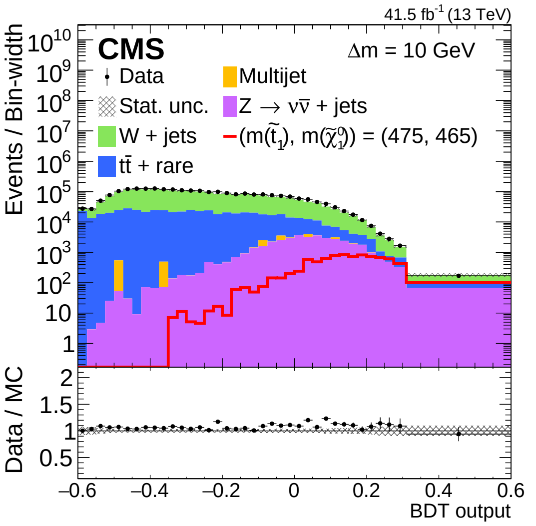

Figure 4: BDT output from 2017 data and MC for $\Delta m = 10$ GeV, with an overlaid signal $(m(\tilde{t}_1), m(\tilde{\chi}_1^0))$ point. The lower panel shows the ratio of data to the background. From [23].

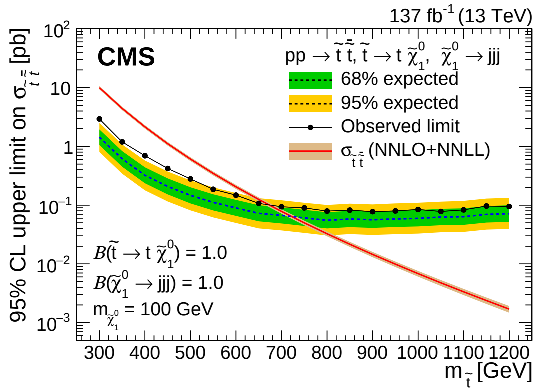

Figure 5: Expected and observed 95% CL upper limit on the $\tilde{t}_1$ production cross section as a function of the top squark mass for the RPV SUSY model. Particle masses and branching fractions assumed for the model are included. The expected cross section is shown in the red curve. From [25].

The observed number of events is consistent with the predicted SM backgrounds in all signal regions. Upper limits are set at the 95% CL on the $\tilde{t}_1\tilde{t}_1$ production cross section as a function of the $\tilde{t}_1$ and $\tilde{\chi}_1^0$ masses, within the context of a simplified model. Assuming a 100% branching fraction in the four-body decay mode, the search excludes top squark masses up to 480 and 700 GeV at $\Delta m = 10$ and 80 GeV, respectively. These results are among the best limits to date on the top squark pair production cross section, where the top squark decays via the four-body mode, and currently correspond to the most stringent limits for $\Delta m < 30$ GeV.

2.4 RPV and stealth SUSY in $E_{\rm T}^{\rm miss}$-agnostic analysis

R-parity is defined as $R = (-1)^{3(B-L)+2S}$, where B (L) is the baryon (lepton) number and S the spin, respectively, granting $R = +1$ ($R = -1$) to all SM particles (SUSY partners) [26]. It is stressed that RPC is merely an *ad-hoc* assumption with the only strict limitation coming from the proton lifetime: non-conservation of both B and L leads to a rapid proton decay. RPC has serious consequences in SUSY phenomenology in colliders: the SUSY particles are produced in pairs and, most importantly, the LSP is absolutely stable, providing the characteristic high $E_{\rm T}^{\rm miss}$ in SUSY events at colliders. If the RPV coupling is sufficiently small, the decay of the LSP into SM particles may be delayed, leading to distinctive signatures discussed in Section 4.1.

A first of its kind CMS search for top squark pair production with subsequent decay characterised by two top quarks, additional gluons or light-flavour quarks, and low $E_{\mathrm{T}}^{\mathrm{miss}}$ is described in Ref. [25]. Events containing exactly one electron or muon and at least seven jets, of which at least one should be b-tagged, are selected from a CMS data sample. No requirement is made on $E_{\mathrm{T}}^{\mathrm{miss}}$. The dominant $t\bar{t}$ background is predicted from data using a simultaneous fit of the jet multiplicity distribution across four bins of a neural network score.

The results are interpreted in terms of top squark pair production in the context of an RPV and the stealth SUSY models. Top squark masses ($\tilde{t}$) up to 670 GeV are excluded at 95% CL for the RPV model in which the top squark decays to a top quark and the lightest neutralino, which subsequently decays to three light-flavour quarks via an off-shell squark through a trilinear coupling λ''. Top squark masses up to 870 GeV are excluded for the stealth SUSY model in which the top squark decays to a top quark, three gluons, and a gravitino via intermediate hidden-sector particles. The maximum observed local significance is 2.8σ corresponding to a best fit signal strength of 0.21 ± 0.07 for the RPV model with $m_{\tilde{t}} = 400$ GeV, making the observed limit weaker than the expected, as shown in Figure 5. A similar analysis has been conducted by ATLAS considering gluino, stop, or electroweakino pair production in RPV SUSY scenarios [27].

3. Electroweak production

Electroweak SUSY production is motivated by naturalness [5, 12] and it is complementary to searches focusing on strongly produced sparticles. Natural models of SUSY favour light chargino and neutralino masses, in a range well accessible at the LHC. In the event that the strong production is sufficiently suppressed due to heavy squarks and gluinos, EW SUSY production may be the dominant SUSY production mechanism at the LHC.

3.1 Two-lepton channel with $E_{\mathrm{T}}^{\mathrm{miss}}$ and no jets and WW fiducial measurement

ATLAS carried out a search for the EW production of charginos and sleptons decaying into final states containing two leptons with opposite electric charge and $E_{\mathrm{T}}^{\mathrm{miss}}$ [28]. Two scenarios are considered: the direct production of slepton pairs, where each slepton decays directly into the lightest neutralino and a lepton, and the production of lightest chargino pairs, where each decays into a final state with the lightest neutralino plus a lepton via a W boson decay. The regions with mass differences up to approximately 150 GeV between the sleptons and neutralino and between the chargino and neutralino are explored in these analyses. Models with smuon production with mass differences in this region of the $m(\tilde{\mu}) - m(\tilde{\chi}_1^0)$ plane are favoured to explain the $(g-2)_\mu$ anomaly for small $\tan\beta$ values, as discussed in Ref. [29]. Their decay topologies are similar to those of SM processes, making it challenging to separate signal from background. In order to target these models, a data-driven technique is used to estimate the main backgrounds in the slepton search, and a semi-data-driven approach using CRs to normalise the main backgrounds, classified with a BDT, is used in the chargino search.

The data are found to be consistent with the SM predictions, and exclusion limits at 95% CL are set on the masses of relevant sparticles in each of these scenarios. Slepton masses up to

150 GeV are excluded in the case of a 50 GeV mass-splitting between the sleptons and neutralino, thus surpassing the exclusion limits previously set by the LEP experiments. Chargino masses up to 140 GeV are excluded in the case of a mass splitting between the chargino and neutralino as low as about 100 GeV, as demonstrated in Figure 6. Compared to previous analyses for the same scenarios, in the regions with a mass difference up to about 150 GeV between the slepton or chargino and neutralino, the results of these searches extend beyond the exclusion limits previously set by ATLAS [30, 31] and CMS [32].

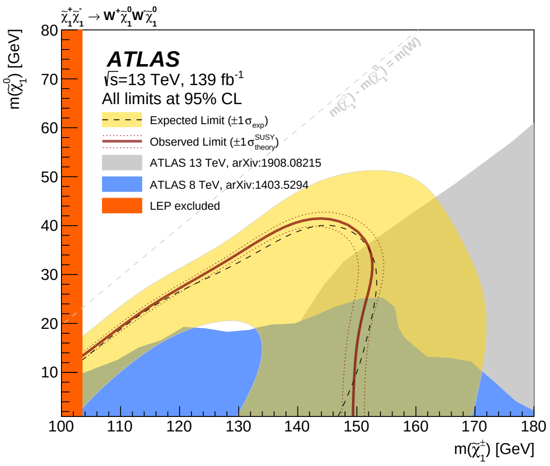

Figure 6: Observed and expected 95% CL exclusion limits for chargino-pair production with W-mediated decays in the $m(\tilde{\chi}_1^{\pm}) - m(\tilde{\chi}_1^0)$ plane. The yellow band around the dashed line corresponds to the $\pm 1\sigma$ variations of the expected limit. The dotted lines around the observed limit illustrate the signal cross-section uncertainty. The observed limits obtained by the ATLAS experiment in previous searches [30, 31] are also shown. From [28].

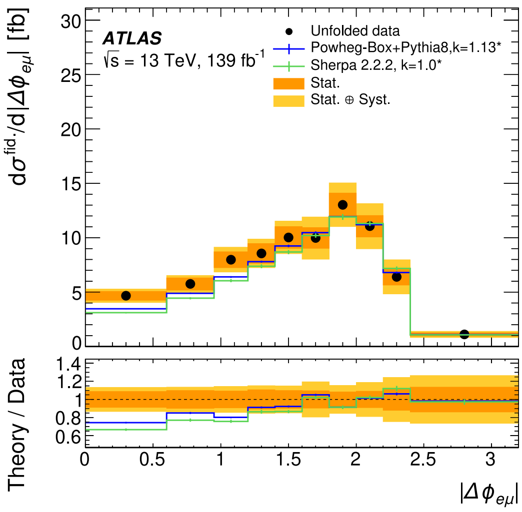

Figure 7: Measured fiducial differential cross-sections of WW production for $|\Delta\phi_{e\mu}|$. The measured values are shown as points with dark (light) bands giving the statistical (total) uncertainty. The results are compared with predictions from various packages with k-factors applied to scale the predictions of qq-initiated (gg-initiated) processes. From [33].

The aforementioned analysis [28] leads to the cross-section measurement [33] for $WW \to e^{\pm}\nu\mu^{\mp}\nu$ production in a fiducial phase-space characterised by the absence of jets and additional leptons, the presence of a high dilepton invariant mass $m_{e\mu}$ and large values of $E_{\mathrm{T}}^{\mathrm{miss}}$ and stransverse mass, M_{T2} [34, 35]. The measured cross section is $\sigma(WW \to e^{\pm}\nu\mu^{\mp}\nu) = 19.2 \pm 0.3\,(\text{stat}) \pm 2.5\,(\text{syst}) \pm 0.4\,(\text{lumi})$ fb. Differential cross sections for three variables sensitive to the energy scale of the event and three variables sensitive to the angular correlations of the leptonic decay products are compared with two theoretical SM predictions from perturbative QCD calculations. Good agreement is observed for most distributions within the uncertainties. The largest discrepancies occur at low values of $|\Delta\phi_{e\mu}| < 1.5$, as seen in Figure 7, which is consistent with the observations of the previous atlas WW+0-jet measurement [36]. This study validates the SM in a new and interesting region motivated particularly by SUSY searches and provides benchmark measurements that can be used to improve future SM predictions and calculate additional constraints on BSM models.

3.2 Final state with two same-sign leptons or three leptons

In the SM, the production of multiple jets in conjunction with two same-sign (SS) or three charged leptons is a very rare process in proton–proton collisions. Therefore, these final states provide a promising starting point in the search for BSM physics [37–42]. ATLAS has recently performed a search for directly produced electroweak gauginos and higgsinos in events with two electrons or muons of the same charge or three leptons [43]. Events were categorised according to the number of jets, b-jets, the $E_{\mathrm{T}}^{\mathrm{miss}}$, the effective mass and other relevant observables, improving substantially the sensitivity to specific RPC and RPV SUSY scenarios. The distribution of the $E_{\mathrm{T}}^{\mathrm{miss}}$ significance, $\mathcal{S}(E_{\mathrm{T}}^{\mathrm{miss}})$, for the low-$M_{\mathrm{T2}}$ SR is shown in Figure 8.

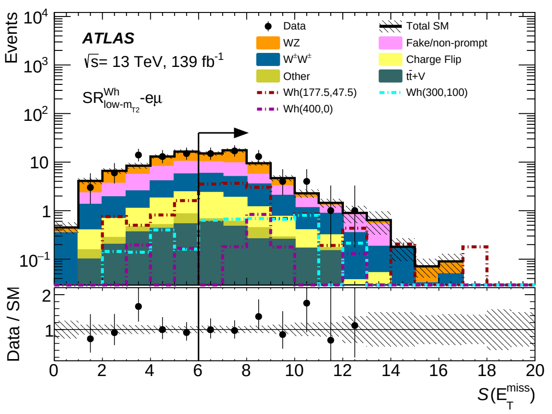

Figure 8: $\mathcal{S}(E_{\mathrm{T}}^{\mathrm{miss}})$ distributions of the data and the expected background in the $e\mu$ channel. Distribution for three Wh signal mass points are overlaid. The bottom panel shows the ratio of data to the predicted yields. The hatched bands indicate the combined theoretical, experimental, data-driven and MC statistical uncertainties. From [43].

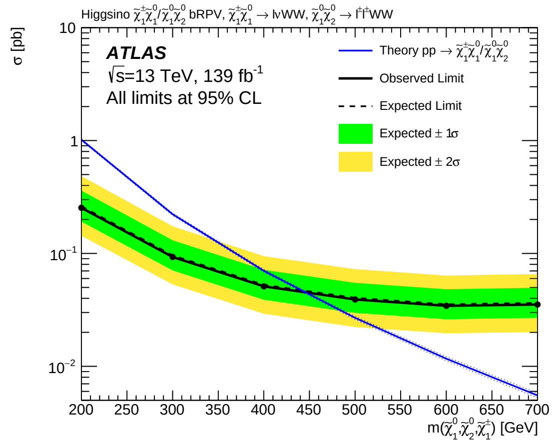

Figure 9: Observed and expected 95% CL exclusion limits as a function of higgsino $\tilde{\chi}_1^0/\tilde{\chi}_2^0/\tilde{\chi}_1^{\pm}$ mass in the bilinear RPV model. The green (yellow) bands around the expected limit express the $\pm 1\sigma$ ($\pm 2\sigma$) uncertainties. The theoretical production cross section is also shown with its uncertainty. From [43].

No significant excess over the expected background is seen. Observed 95% CL limits on the visible cross-section are placed in the defined signal regions and constraints have been set on the parameters of the simplified topologies and complete models considered. In a wino-bino Wh-mediated model, NLSP masses of up to 525 GeV have been excluded for a massless lightest neutralino, extending considerably previous limits set by ATLAS [44] with a 36.1 fb^{-1} dataset and CMS [45] with a 137 fb^{-1} sample of 240 GeV and 300 GeV, respectively. The analogous excluded $\tilde{\chi}_1^{\pm}/\tilde{\chi}_2^0$ mass range for the WZ topology is between 190 GeV and 260 GeV in a channel probed for the first time in ATLAS in the two-SS-lepton final state. In a natural RPV model with bilinear terms [46], never explored before in electroweak SUSY production, mass-degenerate higgsinos $\tilde{\chi}_1^0/\tilde{\chi}_2^0/\tilde{\chi}_1^{\pm}$ lighter than 440 GeV have been excluded, as depicted in Figure 9. Model-independent production cross-section upper bounds as low as 40 ab have been set in signal regions inspired by an RPV baryon-number-violating scenario. Search regions orthogonal to other ATLAS analyses have been deployed in all considered models, improving future statistical combinations with other channels.

3.3 Fully hadronic channel with WX intermediate production

A search for signatures of electroweak production of charginos and neutralinos in fully hadronic final states has been carried out by CMS [47], following a similar analysis by ATLAS [48]. The charginos are assumed to decay to the W boson and the lightest neutralino $\tilde{\chi}_1^0$, and the heavier neutralinos ($\tilde{\chi}_2^0$ and $\tilde{\chi}_3^0$) are assumed to decay to either the Z or the Higgs boson, H, and the $\tilde{\chi}_1^0$. The decay products of W, Z, or Higgs bosons are clustered into large-radius jets. These jets are categorised based on their mass and a collection of novel jet-tagging algorithms based on deep neural networks. Four search regions, three that require b-jets and one that excludes b-jets, are constructed to look for chargino- and neutralino-mediated production of a pair of bosons, WW, WZ, or WH, together with a large $E_{\mathrm{T}}^{\mathrm{miss}}$, as shown in Figure 10. Simplified models are considered in which the charginos $\tilde{\chi}_1^{\pm}$ and the next-to-lightest-neutralino $\tilde{\chi}_2^0$ are assumed to be the mass-degenerate NLSPs. The lightest neutralino $\tilde{\chi}_1^0$ is assumed to be the bino-like LSP.

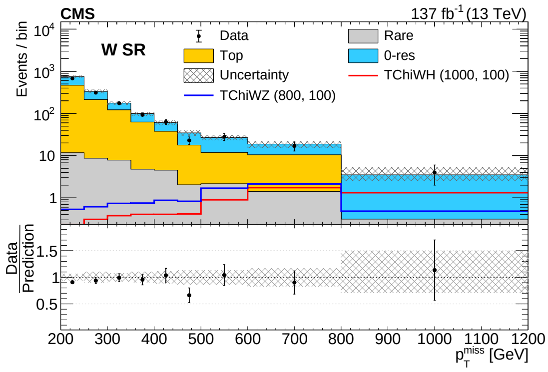

Figure 10: SM background prediction vs. observation in the W SR. The filled stacked histograms show the SM background predictions. The superimposed open histograms show the expectations for selected signal models, denoted in the legend by the name of the model followed by the assumed masses of the NLSP and LSP in GeV. From [47].

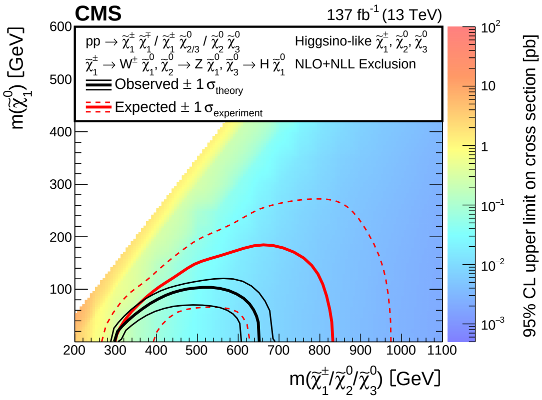

Figure 11: Expected and observed 95% CL exclusion for mass-degenerate higgsino $\tilde{\chi}_1^{\pm}\tilde{\chi}_1^{\mp}$, $\tilde{\chi}_1^{\pm}\tilde{\chi}_2^0$, $\tilde{\chi}_1^{\pm}\tilde{\chi}_3^0$, and $\tilde{\chi}_2^0\tilde{\chi}_3^0$ production as functions of the NLSP and LSP masses. The 95% CL upper limits on the production cross sections are also shown. From [47].

No statistically significant excess of events is observed in the data with respect to the SM expectation. Using wino-like pair production cross sections, 95% CL mass exclusions are derived. For signals with WW, WZ, or WH boson pairs, the NLSP mass exclusion limit for low-mass LSPs extends up to 670, 760, and 970 GeV, respectively. When we consider models including both wino-like NLSP $\tilde{\chi}_1^{\pm}\tilde{\chi}_2^0$ and $\tilde{\chi}_1^{\pm}\tilde{\chi}_1^{\mp}$ production under the assumption that either $\tilde{\chi}_2^0 \to Z\tilde{\chi}_1^0$ or $\tilde{\chi}_2^0 \to H\tilde{\chi}_1^0$, the NLSP mass exclusion extends up to 870 and 960 GeV, respectively. Alternatively, with higgsino-like NLSPs $\tilde{\chi}_1^{\pm}$, $\tilde{\chi}_2^0$, and $\tilde{\chi}_3^0$, the higgsino masses from 300 to 650 GeV are excluded for low-mass LSPs, as observed in Figure 11. These mass exclusions significantly improve on those achieved by searches using leptonic probes of SUSY for high NLSP masses.

3.4 Tau slepton pairs

A search for direct τ slepton $\tilde{\tau}$ pair production has been performed by CMS in events with two hadronically decaying τ leptons, τ_{h}, and significant $E_{\mathrm{T}}^{\mathrm{miss}}$ [49]. Both prompt and displaced decays of the τ slepton are considered. Thirty-one different search regions are used in the analysis, based on kinematic observables that exploit expected differences between signal and background. No significant excess of events above the expected standard model background has been observed. Upper limits have been set on the cross section for direct $\tilde{\tau}$ pair production for simplified models in which each $\tilde{\tau}$ decays to a τ lepton and the LSP. For purely left-handed $\tilde{\tau}$ pair production with prompt decays, $\tilde{\tau}$ masses between 115 and 340 GeV are excluded at 95% CL for a nearly massless LSP, while for the degenerate production of left- and right-handed $\tilde{\tau}$ pairs, $\tilde{\tau}$ masses up to 400 GeV are excluded under the same hypothesis. The limits observed are the most stringent obtained thus far in the case of direct $\tilde{\tau}$ pair production with prompt $\tilde{\tau}$ decays, for both the purely left-handed and degenerate production scenarios. They represent a considerable improvement in sensitivity with respect to a previous CMS search [50]. In the context of long-lived τ sleptons, final states with displaced $\tau_{\rm h}$ candidates are investigated for the first time. In a scenario with $c\tau_0 = 0.1$ mm, where τ_0 denotes the mean proper lifetime of the $\tilde{\tau}$, masses between 150 and 220 GeV are excluded for the case that the LSP is nearly massless, as shown in Figure 12.

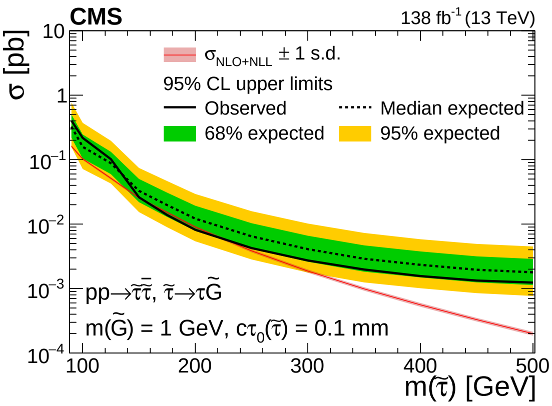

Figure 12: Expected and observed 95% CL cross section upper limits as functions of the $\tilde{\tau}$ mass for long-lived $\tilde{\tau}$ in the maximally mixed scenario for an LSP mass of 1 GeV, and for $c\tau_0$ values of 0.1 mm. The green (yellow) band indicates the regions containing 68% (95%) of the distribution of limits expected under the background-only hypothesis. The prediction for the signal production cross section and its uncertainty is also shown. From [49].

4. Long-lived particles

In some supersymmetric theoretical scenarios, the existence of long-lived particles (LLPs) is predicted [51], that may either decay within the typical volume of an LHC detector or may traverse it entirely as (meta)stable. In the former case, it may give rise to displaced vertices, disappearing tracks or other signatures. On the other hand, heavy stable charged particles can be probed though the anomalous ionisation that they give rise to. The general-purpose ATLAS and CMS experiments at the LHC are searching for and have set limits in LLP scenarios [52, 53]. Besides them, dedicated detectors are being proposed to explore these less-constrained manifestations of BSM physics [53].

4.1 Displaced vertices

A search for BSM physics giving rise to LLP decays into hadrons has been performed by ATLAS [54] using events that contain multiple energetic jets and a displaced vertex (DV). Similar searches were performed previously by the ATLAS [55–58] and CMS collaborations [59, 60]. Event selections are developed to efficiently reject backgrounds. The yields expected from background in the two orthogonal SRs used in the analysis are extracted from data. The data agree with the yields expected from the background-only hypothesis, with zero and one event passing the trackless and high-p_T jet SR requirements, respectively; the former data-versus-MC distributions is given in Figure 13.

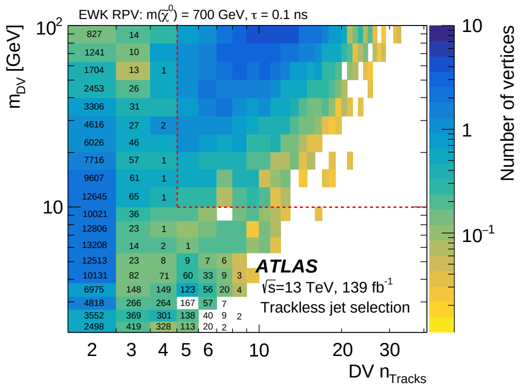

Figure 13: Invariant mass m_{DV} and track multiplicity for DVs in events with trackless jet selection requirements. The observed vertex yields in data are shown, while the colours express the expected signal yield of an RPV model. The dashed line shows the SR definition. From [54].

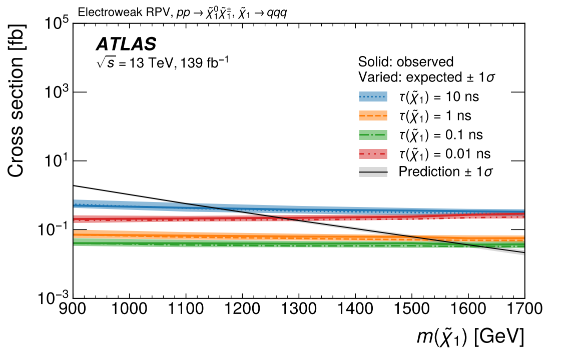

Figure 14: Exclusion limits at 95% CL on the production cross section of electroweakino pairs in the EWK RPV model as a function of $m(\tilde{\chi}_1^0)$ are shown for several values of $\tau(\tilde{\chi}_1^0)$. The theoretical prediction of the signal production cross section and its uncertainty are shown in grey. From [54].

The results are interpreted in SUSY models with electroweakinos decaying via small values of the RPV couplings λ'' into quarks giving the electroweakinos lifetimes τ in the picosecond to nanosecond range. At 95% CL, $m(\tilde{\chi}_1^0)$ values up to 1.58 TeV for $\tau = 0.1$ ns are excluded independently of the presence of a heavier gluino, as becomes evident from Figure 14. Upper limits on the visible cross section for processes with the sought signature are also derived to be 0.03 fb and 0.02 fb for the high-p_T jet and trackless jet SRs, respectively. This analysis significantly expands the limits given by previous ATLAS searches [57].

4.2 Non-pointing photons

A search has been performed by ATLAS for delayed and non-pointing photons produced from exotic decays of the 125 GeV Higgs boson into a pair of BSM LLPs such as the NLSP present in GMSB models [61]. The analysis uses measurements of the trajectories and arrival times (cf. Figure 15) of photons in the ATLAS liquid-Argon electromagnetic calorimeter to search for possible displaced photons.

No excess is observed above the expectation from prompt background processes which are modelled entirely using data control samples. The results are used to set limits on $\mathcal{B}(H \to \text{NLSP NLSP})$ for NLSP lifetimes ranging from 0.25 ns to 100 ns, assuming that $\mathcal{B}(\text{NLSP} \to \text{LSP} + \gamma = 100\%$. The limits are determined in a two-dimensional grid of NSLP mass values from 30 GeV to 60 GeV and LSP masses from 0.5 GeV up to $m_{\text{NLSP}} - 10$ GeV. The most stringent constraints limit $\mathcal{B}(H \to \text{NLSP NLSP})$ to less than about 1% for intermediate NLSP lifetime values and for the largest NLSP mass and mass-splitting between the NLSP and LSP. A model-independent limit is also set on the production of photons with large values of displacement and time delay.

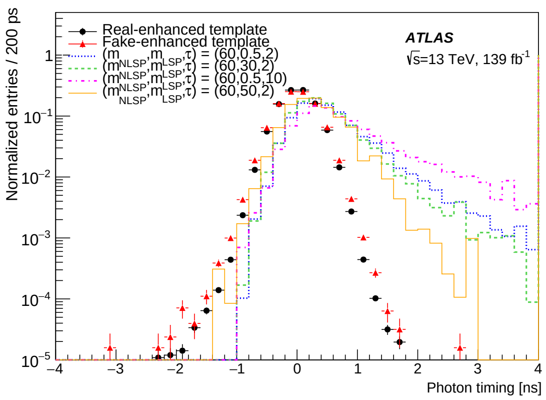

Figure 15: Photon timing distributions for the genuine-photon enriched and fake-photon enriched samples. Superimposed are the expected distributions for selected signal models. The signal models are labeled by the values of their NLSP and LSP masses (m_{NLSP} and m_{LSP} in GeV) and NLSP lifetime (τ in ns). From [61].

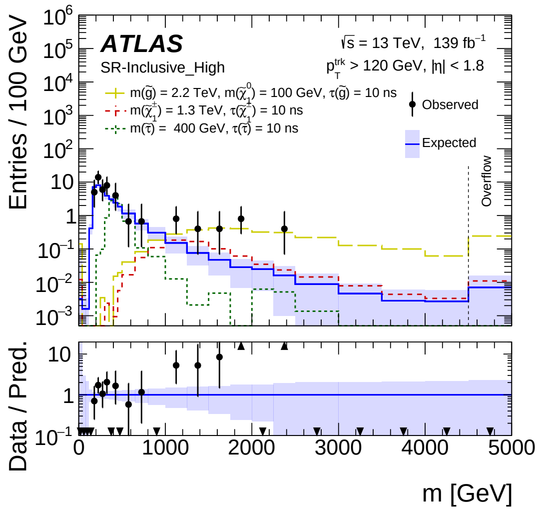

Figure 16: Observed mass distribution in the inclusive-high SR. The band on the expected background indicates the total uncertainty. Several representative signal models are overlaid. From [62].

4.3 Large ionisation energy loss

A search has been performed in ATLAS for heavy charged LLPs, with lifetimes sufficient $\tau \lesssim 1$ ns to reconstruct inner-detector tracks [62]. The identification of LLPs is based on anomalously high specific ionisation measured by the ATLAS pixel detector for isolated high-p_{T} tracks in events with high $E_{\text{T}}^{\text{miss}}$. The considerable increase in sensitivity compared to previous ATLAS searches is not only due to the higher integrated luminosity, but also to several significant improvements in the analysis strategy. The most noticeable are the use of a higher $\mathrm{d}E/\mathrm{d}x$ threshold, the separate treatment of the tracks with an IBL overflow flag and the use of a data-driven $\mathrm{d}E/\mathrm{d}x$-response template instead of a simulated one, as well as a more optimised definition of sub-regions in the SR for exclusion interpretations. Evaluation of systematic uncertainties was also improved through the adoption of a high-p_{T} validation region and the implementation of a pseudo-SR to test the background generation method.

Observed yields and distributions agree with the SM background expectations, with the exception of an accumulation of events in the high-$\mathrm{d}E/\mathrm{d}x$ and high-mass range, shown in Figure 16. The local (global) significance of this excess is 3.6σ (3.3σ) in a sub-range of the signal region optimised for a target mass hypothesis of 1.4 TeV. The events in the excess region were examined in detail, although no obvious pathologies were identified in the measurement of these events. The time-of-flight measurements in outer detector subsystems clearly indicate that none of the candidate tracks are from charged particles moving significantly slower than the speed of light.

Maximum sensitivity is reached for LLPs with lifetimes of around 10–30 ns. Masses smaller than 2.27 TeV are excluded at the 95% CL for gluino R-hadrons with a lifetime of 20 ns and $m(\tilde{\chi}_1^0) = 100$ GeV. The mass limit for compressed-scenario R-hadrons, with $\Delta m(\tilde{g}, \tilde{\chi}_1^0) = 30$ GeV and a lifetime of 30 ns, is 2.06 TeV. Masses below 1.07 TeV for charginos and in the range 220–360 GeV for $\tilde{\tau}$'s are excluded for lifetimes of 30 ns and 10 ns, respectively. The limits in the mass–lifetime plane are the most stringent to date and provide further constraints on the R-hadron, chargino and $\tilde{\tau}$ production models considered.

5. Summary and outlook

Supersymmetry signals have been extensively sought after by the ATLAS and CMS experiments, motivated by various theoretical approaches, models and topologies: strong production, including 3$^{\text{rd}}$-generation fermions, electroweak production, R-parity violation, delayed decays, high ionisation, among others. They lead to a wide spectrum of signatures: $E_{\mathrm{T}}^{\mathrm{miss}}$ + jets + leptons / photons / b-jets/ τ-leptons, displaced vertices, and it is not possible to cover all of them here. No significant deviation from known SM processes has been observed up to now with the data collected during LHC Run 2 at $\sqrt{s}$ = 13 TeV. In view of the null results in *conventional* SUSY searches, it becomes necessary to fully explore *non-standard* SUSY scenarios also involving RPV and/or quasi-stable particles.

As both experimental techniques and search strategies keep evolving, ATLAS and CMS keep looking for supersymmetry with the new data that become available at the LHC, in particular the proton–proton collision data at $\sqrt{s}$ = 13.6 TeV that are being collected in LHC Run 3 that started in 2022. Summary plots of most recent results are continuously updated in Refs. [63, 64].

Acknowledgments

The author thanks the Corfu2022 organisers for the kind invitation. She acknowledges support by the Generalitat Valenciana via the Excellence Grant CIPROM/2021/073 and the mobility grant CIBEST/2021/29, by the Spanish MICIU / AEI and the European Union / FEDER via the grants PGC2018-094856-B-I00 and PID2021-122134NB-C21, and by CSIC via the grant 2021AEP063.

References

[1] J. Wess and B. Zumino, A. Salam and E. Sezgin, eds., *Supergauge Transformations in Four Dimensions*, *Nucl. Phys. B* **70** (1974) 39.

[2] A. Salam and J. A. Strathdee, *Supersymmetry and Nonabelian Gauges*, *Phys. Lett. B* **51** (1974) 353.

[3] S. Ferrara and B. Zumino, *Supergauge Invariant Yang-Mills Theories*, *Nucl. Phys. B* **79** (1974) 413.

[4] S. P. Martin, G. L. Kane, ed., *A Supersymmetry primer*, *Adv. Ser. Direct. High Energy Phys.* **18** (1998) 1 [hep-ph/9709356].

[5] B. de Carlos and J. A. Casas, *One loop analysis of the electroweak breaking in supersymmetric models and the fine tuning problem*, *Phys. Lett. B* **309** (1993) 320 [hep-ph/9303291].

[6] V. A. Mitsou, *Shedding Light on Dark Matter at Colliders*, *Int. J. Mod. Phys. A* **28** (2013) 1330052 [1310.1072].

[7] J. R. Ellis, L. E. Ibanez and G. G. Ross, *Grand Unification with Large Supersymmetry Breaking*, *Phys. Lett. B* **113** (1982) 283.

[8] LHC Reinterpretation Forum collaboration, *Reinterpretation of LHC Results for New Physics: Status and Recommendations after Run 2*, *SciPost Phys.* **9** (2020) 022 [2003.07868].

[9] ATLAS collaboration, *The ATLAS Experiment at the CERN Large Hadron Collider*, *JINST* **3** (2008) S08003.

[10] CMS collaboration, *The CMS Experiment at the CERN LHC*, *JINST* **3** (2008) S08004.

[11] L. Evans and P. Bryant, eds., *LHC Machine*, *JINST* **3** (2008) S08001.

[12] R. Barbieri and G. F. Giudice, *Upper Bounds on Supersymmetric Particle Masses*, *Nucl. Phys. B* **306** (1988) 63.

[13] CMS collaboration, *Search for supersymmetry in final states with a single electron or muon using angular correlations and heavy-object identification in proton-proton collisions at $\sqrt{s}$ = 13 TeV*, 2211.08476.

[14] CMS collaboration, *Search for supersymmetry in events with one lepton and multiple jets exploiting the angular correlation between the lepton and the missing transverse momentum in proton-proton collisions at $\sqrt{s}$ = 13 TeV*, *Phys. Lett. B* **780** (2018) 384 [1709.09814].

[15] ATLAS collaboration, *Search for squarks and gluinos in final states with one isolated lepton, jets, and missing transverse momentum at $\sqrt{s}$ = 13 TeV with the ATLAS detector*, *Eur. Phys. J. C* **81** (2021) 600 [2101.01629].

[16] ATLAS collaboration, *Searches for new phenomena in events with two leptons, jets, and missing transverse momentum in 139 fb^{-1} of $\sqrt{s}$ = 13 TeV pp collisions with the ATLAS detector*, *Eur. Phys. J. C* **83** (2023) 515 [2204.13072].

[17] M. E. Cabrera, J. A. Casas, V. A. Mitsou, R. Ruiz de Austri and J. Terron, *Histogram comparison as a powerful tool for the search of new physics at LHC. Application to CMSSM*, *JHEP* **04** (2012) 133 [1109.3759].

[18] ATLAS collaboration, *Search for chargino-neutralino production using recursive jigsaw reconstruction in final states with two or three charged leptons in proton-proton collisions at $\sqrt{s}$ = 13 TeV with the ATLAS detector*, *Phys. Rev. D* **98** (2018) 092012 [1806.02293].

[19] ATLAS collaboration, *Search for supersymmetry in events containing a same-flavour opposite-sign dilepton pair, jets, and large missing transverse momentum in $\sqrt{s}$ = 8 TeV pp collisions with the ATLAS detector*, *Eur. Phys. J. C* **75** (2015) 318 [1503.03290].

[20] ATLAS collaboration, *Search for new phenomena in events containing a same-flavour opposite-sign dilepton pair, jets, and large missing transverse momentum in $\sqrt{s}$ = 13 TeV pp collisions with the ATLAS detector*, *Eur. Phys. J. C* **77** (2017) 144 [1611.05791].

[21] ATLAS collaboration, *Search for new phenomena using the invariant mass distribution of same-flavour opposite-sign dilepton pairs in events with missing transverse momentum in $\sqrt{s}$ = 13 TeV pp collisions with the ATLAS detector*, *Eur. Phys. J. C* **78** (2018) 625 [1805.11381].

[22] CMS collaboration, *Search for supersymmetry in final states with two oppositely charged same-flavor leptons and missing transverse momentum in proton-proton collisions at $\sqrt{s}$ = 13 TeV*, *JHEP* **04** (2021) 123 [2012.08600].

[23] CMS collaboration, *Search for top squarks in the four-body decay mode with single lepton final states in proton-proton collisions at $\sqrt{s}$ = 13 TeV*, *JHEP* **06** (2023) 060 [2301.08096].

[24] CMS collaboration, *Search for top squarks decaying via four-body or chargino-mediated modes in single-lepton final states in proton-proton collisions at $\sqrt{s}$ = 13 TeV*, *JHEP* **09** (2018) 065 [1805.05784].

[25] CMS collaboration, *Search for top squarks in final states with two top quarks and several light-flavor jets in proton-proton collisions at $\sqrt{s}$ = 13 TeV*, *Phys. Rev. D* **104** (2021) 032006 [2102.06976].

[26] H. K. Dreiner, G. L. Kane, ed., *An Introduction to explicit R-parity violation*, *Adv. Ser. Direct. High Energy Phys.* **21** (2010) 565 [hep-ph/9707435].

[27] ATLAS collaboration, *Search for R-parity-violating supersymmetry in a final state containing leptons and many jets with the ATLAS experiment using $\sqrt{s}$ = 13 TeV proton–proton collision data*, *Eur. Phys.*

J. C **81** (2021) 1023 [2106.09609].

[28] ATLAS collaboration, *Search for direct pair production of sleptons and charginos decaying to two leptons and neutralinos with mass splittings near the W-boson mass in $\sqrt{s}$ = 13 TeV pp collisions with the ATLAS detector*, *JHEP* **06** (2023) 031 [2209.13935].

[29] ATLAS collaboration, *SUSY Summary Plots March 2022*, ATL-PHYS-PUB-2022-013, http://cds.cern.ch/record/2805985, 2022.

[30] ATLAS collaboration, *Search for direct production of charginos, neutralinos and sleptons in final states with two leptons and missing transverse momentum in pp collisions at $\sqrt{s}$ = 8 TeV with the ATLAS detector*, *JHEP* **05** (2014) 071 [1403.5294].

[31] ATLAS collaboration, *Search for electroweak production of charginos and sleptons decaying into final states with two leptons and missing transverse momentum in $\sqrt{s}$ = 13 TeV pp collisions using the ATLAS detector*, *Eur. Phys. J. C* **80** (2020) 123 [1908.08215].

[32] CMS collaboration, *Combined search for electroweak production of charginos and neutralinos in proton-proton collisions at $\sqrt{s}$ = 13 TeV*, *JHEP* **03** (2018) 160 [1801.03957].

[33] ATLAS collaboration, *Measurements of W^+W^- production in decay topologies inspired by searches for electroweak supersymmetry*, 2206.15231.

[34] C. G. Lester and D. J. Summers, *Measuring masses of semiinvisibly decaying particles pair produced at hadron colliders*, *Phys. Lett. B* **463** (1999) 99 [hep-ph/9906349].

[35] C. G. Lester, *The stransverse mass, MT2, in special cases*, *JHEP* **05** (2011) 076 [1103.5682].

[36] ATLAS collaboration, *Measurement of fiducial and differential W^+W^- production cross-sections at $\sqrt{s}$ = 13 TeV with the ATLAS detector*, *Eur. Phys. J. C* **79** (2019) 884 [1905.04242].

[37] ATLAS collaboration, *Search for supersymmetry at $\sqrt{s}$ = 8 TeV in final states with jets and two same-sign leptons or three leptons with the ATLAS detector*, *JHEP* **06** (2014) 035 [1404.2500].

[38] ATLAS collaboration, *Search for supersymmetry at $\sqrt{s}$ = 13 TeV in final states with jets and two same-sign leptons or three leptons with the ATLAS detector*, *Eur. Phys. J. C* **76** (2016) 259 [1602.09058].

[39] ATLAS collaboration, *Search for supersymmetry in final states with two same-sign or three leptons and jets using 36 fb^{-1} of $\sqrt{s}$ = 13 TeV pp collision data with the ATLAS detector*, *JHEP* **09** (2017) 084 [1706.03731].

[40] ATLAS collaboration, *Search for squarks and gluinos in final states with same-sign leptons and jets using 139 fb^{-1} of data collected with the ATLAS detector*, *JHEP* **06** (2020) 046 [1909.08457].

[41] CMS collaboration, *Search for physics beyond the standard model in events with two leptons of same sign, missing transverse momentum, and jets in proton–proton collisions at $\sqrt{s}$ = 13 TeV*, *Eur. Phys. J. C* **77** (2017) 578 [1704.07323].

[42] CMS collaboration, *Search for physics beyond the standard model in events with jets and two same-sign or at least three charged leptons in proton-proton collisions at $\sqrt{s}$ = 13 TeV*, *Eur. Phys. J. C* **80** (2020) 752 [2001.10086].

[43] ATLAS collaboration, *Search for direct production of winos and higgsinos in events with two same-charge leptons or three leptons in pp collision data at $\sqrt{s}$ = 13 TeV with the ATLAS detector*, 2305.09322.

[44] ATLAS collaboration, *Search for chargino and neutralino production in final states with a Higgs boson and missing transverse momentum at $\sqrt{s}$ = 13 TeV with the ATLAS detector*, *Phys. Rev. D* **100** (2019) 012006 [1812.09432].

[45] CMS collaboration, *Search for electroweak production of charginos and neutralinos in proton-proton collisions at $\sqrt{s}$ = 13 TeV*, *JHEP* **04** (2022) 147 [2106.14246].

[46] ATLAS collaboration, *Constraints on promptly decaying supersymmetric particles with lepton-number- and R-parity-violating interactions using Run-1 ATLAS data*, ATLAS-CONF-2015-018, http://cds.cern.ch/record/2017303, 5, 2015.

[47] CMS collaboration, *Search for electroweak production of charginos and neutralinos at s=13TeV in final states containing hadronic decays of WW, WZ, or WH and missing transverse momentum*, Phys. Lett. B **842** (2023) 137460 [2205.09597].

[48] ATLAS collaboration, *Search for charginos and neutralinos in final states with two boosted hadronically decaying bosons and missing transverse momentum in pp collisions at $\sqrt{s}$ = 13 TeV with the ATLAS detector*, Phys. Rev. D **104** (2021) 112010 [2108.07586].

[49] CMS collaboration, *Search for direct pair production of supersymmetric partners of τ leptons in the final state with two hadronically decaying τ leptons and missing transverse momentum in proton-proton collisions at $\sqrt{s}$ = 13 TeV*, 2207.02254.

[50] CMS collaboration, *Search for direct pair production of supersymmetric partners to the τ lepton in proton-proton collisions at $\sqrt{s}$ = 13 TeV*, Eur. Phys. J. C **80** (2020) 189 [1907.13179].

[51] M. Fairbairn, A. C. Kraan, D. A. Milstead, T. Sjostrand, P. Z. Skands and T. Sloan, *Stable Massive Particles at Colliders*, Phys. Rept. **438** (2007) 1 [hep-ph/0611040].

[52] L. Lee, C. Ohm, A. Soffer and T.-T. Yu, *Collider Searches for Long-Lived Particles Beyond the Standard Model*, Prog. Part. Nucl. Phys. **106** (2019) 210 [1810.12602].

[53] J. Alimena et al., *Searching for long-lived particles beyond the Standard Model at the Large Hadron Collider*, J. Phys. G **47** (2020) 090501 [1903.04497].

[54] ATLAS collaboration, *Search for long-lived, massive particles in events with displaced vertices and multiple jets in pp collisions at $\sqrt{s}$ = 13 TeV with the ATLAS detector*, 2301.13866.

[55] ATLAS collaboration, *Search for displaced vertices arising from decays of new heavy particles in 7 TeV pp collisions at ATLAS*, Phys. Lett. B **707** (2012) 478 [1109.2242].

[56] ATLAS collaboration, *Search for displaced muonic lepton jets from light Higgs boson decay in proton-proton collisions at $\sqrt{s}$ = 7 TeV with the ATLAS detector*, Phys. Lett. B **721** (2013) 32 [1210.0435].

[57] ATLAS collaboration, *Search for massive, long-lived particles using multitrack displaced vertices or displaced lepton pairs in pp collisions at $\sqrt{s}$ = 8 TeV with the ATLAS detector*, Phys. Rev. D **92** (2015) 072004 [1504.05162].

[58] ATLAS collaboration, *Search for long-lived, massive particles in events with a displaced vertex and a muon with large impact parameter in pp collisions at $\sqrt{s}$ = 13 TeV with the ATLAS detector*, Phys. Rev. D **102** (2020) 032006 [2003.11956].

[59] CMS collaboration, *Search for long-lived particles with displaced vertices in multijet events in proton-proton collisions at $\sqrt{s}$ = 13 TeV*, Phys. Rev. D **98** (2018) 092011 [1808.03078].

[60] CMS collaboration, *Search for long-lived particles decaying to jets with displaced vertices in proton-proton collisions at $\sqrt{s}$ = 13 TeV*, Phys. Rev. D **104** (2021) 052011 [2104.13474].

[61] ATLAS collaboration, *Search for displaced photons produced in exotic decays of the Higgs boson using 13 TeV pp collisions with the ATLAS detector*, 2209.01029.

[62] ATLAS collaboration, *Search for heavy, long-lived, charged particles with large ionisation energy loss in pp collisions at $\sqrt{s}$ = 13 TeV using the ATLAS experiment and the full Run 2 dataset*, 2205.06013.

[63] ATLAS collaboration, "Summary plots from the ATLAS Supersymmetry physics group." https://atlas.web.cern.ch/Atlas/GROUPS/PHYSICS/CombinedSummaryPlots/SUSY/, 2023.

[64] CMS collaboration, "CMS SUSY Physics Results." https://twiki.cern.ch/twiki/bin/view/CMSPublic/PhysicsResultsSUS, 2023.